NUKLEONIKA 2012;57(3):323–332 ORIGINAL PAPER

Post acceleration of ions emitted from laser and spark-generated plasmas

Lorenzo Torrisi, Salvadore Cavallaro, Marcin Rosiński, Vincenzo Nassisi, Victor Paperny, Igor Romanov

Abstract. Pulsed lasers at intensities of the order of 10^{10} W/cm^2 interacting with solid matter in vacuum, produce hot plasmas at high temperatures and densities. The charge state distributions of the plasma generate a high electric field, which induces high ion acceleration along the normal to the target surface. The high yield of the emitted ions can generate a near constant current by using repetitive pulses irradiating thick targets. In order to increase ion energy, a post-acceleration system can be employed by using acceleration voltages above 10 kV. Special ion extraction methods can be employed to generate the final ion beam, which is multi-ionic and multi-energetic, due to the presence of different ion species and of different charge states. In this article four different methods of post ion acceleration, employed at the INFN-LNS of Catania, at the IPPLM of Warsaw, at the INFN of Lecce and at the LPI of Moscow, are presented, discussed and compared. All methods are able to implant ions in different substrates at different depth and at different dose-rates.

Key words: post ion acceleration • laser plasma • ion beam • ion implantation

L. Torrisi✉
Dipartimento di Fisica,
Università di Messina,
Ctr. da Papardo-Sperone 31, 98166 Messina, Italy
and Laboratori Nazionali del Sud,
Istituto Nazionale di Fisica Nucleare (INFN)
(National Institute for Nuclear Physics),
62 S. Sofia Str., 95123 Catania, Italy,
Tel.: +39 090 676 5052, Fax: +39 090 39 5400,
E-mail: lorenzo.torrisi@unime.it

S. Cavallaro
Laboratori Nazionali del Sud,
Istituto Nazionale di Fisica Nucleare (INFN)
(National Institute for Nuclear Physics),
62 S. Sofia Str., 95123 Catania, Italy

M. Rosiński
Institute of Plasma Physics and Laser Microfusion,
23 Hery Str., 01-497 Warsaw, Poland

V. Nassisi
Dipartimento di Fisica, Università del Salento,
INFN, Via Arnesano, Lecce, Italy

V. Paperny
Physics Department, Irkutsk State University,
1 K. Marx Str., Irkutsk, 664003, Russia

I. Romanov
P. N. Lebedev Physical Institute, Russian Academy of Sciences,
53 Leninsky Prospect, Moscow, 117924, Russia

Received: 22 November 2011
Accepted: 6 March 2012

Introduction

The plasma generation by short laser pulses initiated a very actual and attractive research field because it permits to generate ion beams without use of expensive and large accelerators. Today at a laser intensities of the order of 10^{20} W/cm^2, it is possible to accelerate ions above 10 MeV per charge state [6].

Laser-generated plasmas accelerate ions along the normal to the target surface. At intensities of the order of $10^{10\div12}$ W/cm^2 and ns pulse duration, laser interacting with solid matter in vacuum produces hot plasmas at high temperature and densities, of the order of $10\div100$ eV and $10^{18\div20}$ electrons/cm^3, respectively [14]. Three mechanisms are responsible for the ion acceleration in plasma, thermal interactions, isothermal and adiabatic expansion in vacuum and Coulomb interactions. Each one can be evaluated as a function of laser irradiation parameters, in agreement with the "Coulomb-Boltzmann-shifted" (CBS) distribution [16]. At 10^{10} W/cm^2, the maximum ion energy is below 1 keV/charge state, thus protons can reach hundreds eV, while fully ionized carbon, C^{6+}, can reach some keV [5, 15].

The low ion energy generally is not sufficient to employ the obtainable ion beams, except for ion sputtering, deposition thin films and laser ion sources. In order to increase the energy of the ions extractable from laser-generated plasma, a post ion acceleration system can be employed. Generally, a voltage of the order of 30–100 kV can be employed to accelerate ions at energies depending on their charge state.

Different methods can be employed to extract the ions from plasma and to submit them to post acceleration towards the final substrate, where the beam collides with atoms of the solid.

The positive polarization of the laser-irradiated target permits to extract ions from the plasma and the use of a high electric field along the emission direction permits to increase the kinetic ion energy.

Due to the multi-atomic species emitted from the target (not only atomic species, but also atoms aggregates, molecules, clusters and contaminants which can be emitted) and due to the different charge states of the ejected ions (the maximum charge state is about 10^+ at 10^{10} W/cm^2), the extracted ion beams are multi-ionic and multi-energetic.

The ion beam production from low laser intensities shows the advantage to be economic, of small dimensions, using high repetitive laser pulses (~10–100 Hz), to be of high reproducibility, thanks to the use of laser repetition rate irradiating roto-translating thick targets to extract a near constant ion current. Other advantages consist in the optimization of the laser pulse parameters (pulse duration, wavelength, focal spot dimension, etc.) and in the use of a low energy laser pulse for initiation of a vacuum discharge (spark) in order to generate reproducible ion beams. These conditions are optimal to reach high current densities, of the order of tens mA/cm^2 [10].

In this article four different methods of post ion acceleration are presented based on: positive polarization of the laser-irradiated target National Institute for Nuclear Physics-Laboratori Nazionali del Sud (INFN-LNS of Catania, Italy); submitting of the ion emission to a local electric field, between two diaphragms, during their flight travel in vacuum Institute of Plasma Physics and Laser Microfusion (IPPLM of Warsaw, Poland); using high electric acceleration inside a little expansion chamber containing three electrodes National Institute for Nuclear Physics (INFN of Lecce, Italy); the use of the so-called 'hot points' or micropinches, due to vacuum discharges (sparks) laser-induced, inside and electric field Lebedev Physical Institute (LPI of Moscow, Russia).

Experimental set-ups

INFN-LNS of Catania

To produce solid target ablation, a Nd:YAG laser with 9 ns laser pulse, operating at a 1064 nm fundamental wavelength, 900 mJ maximum pulsed laser energy, single or 1–30 Hz laser repetition pulses, was employed at the INFN-LNS of Catania. The laser was focused on the target through a lens outside the vacuum chamber (to avoid optics damage due to deposition and implantation of ions and nanoparticles) that, thanks to a pump system, has a vacuum around 1×10^{-6} mbar.

To obtain a post-acceleration, a parallelepiped metallic chamber was used with dimensions of $26 \times 11 \times 11$ cm^3. The target was placed in the centre of the acceleration chamber at the same potential. A metallic rod sustained the target and was capable of changing the target position. A lateral hole permitted the laser to enter inside the chamber and to hit the target at an angle of 43° with respect to the normal surface. A sketch of the extraction chamber is shown in Fig. 1a.

The chamber and the target were connected together with the same electrical potential that can be set between 0 up to +30 kV, by using a high voltage power supply (Yokogawa, 30 kV–200 mA).

The frontal part of the extraction chamber was totally opened, in order to permit the plasma to exit along the normal to the target surface. From this box aperture, an electrical structure of 12 metallic discs all parallel and aligned along to the chamber longitudinal axis, at a distance of 5 mm from each other, with a central hole of 8 mm in diameter, are electrically connected together through 10 MΩ resistors. Assuming to be negligible, the charges imprinting on the discs, the 10 MΩ resistor was sufficient to fed the discs stabilizing the potential. The first disc was connected to the 30 kV positive voltage, while the last disc was connected to the ground. In this way the system generates a uniform accelerating electric field developed at a 60 mm distance. The corresponding maximum acceleration electric field was 5 kV/cm.

Ion collectors (IC) and an electrostatic deflector ion energy analyzer (IEA) are employed in time-of-flight (TOF) configuration in order to detect the integral ion emission and the single ions vs. the charge state. IC gives information on the total current of the post accelerated ions, while IEA gives information on the energy-to-charge state ratio, on the ion charge states, on the ion species and, by changing the electrostatic deflection bias, on the ion energy and charge state distributions.

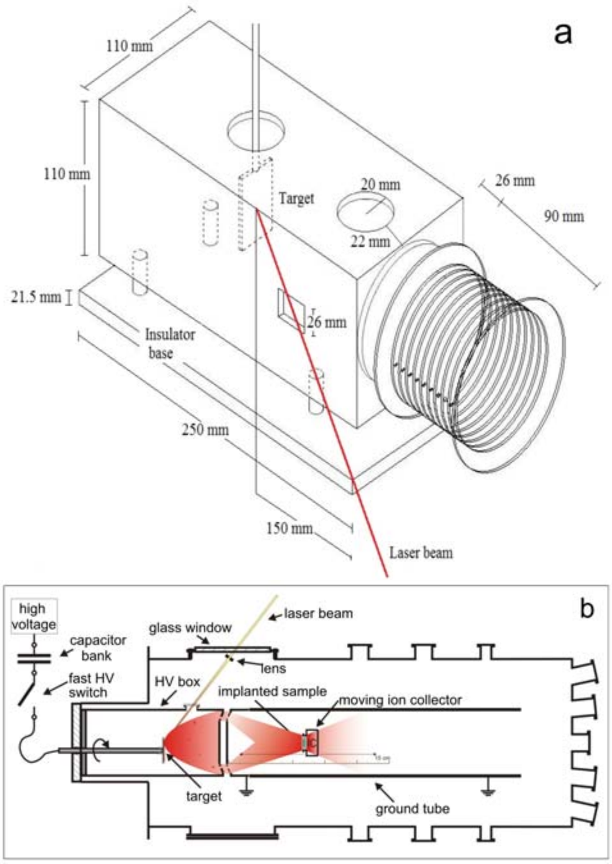

Fig. 1. Scheme of the design of the extraction chamber employed at INFN-LNS of Catania (a) and at IPPLM of Warsaw (b).

Different metallic and plastic targets were used for these experiments, especially Ge, Cu, CH_2 and Ti. At the end of the accelerating system different substrates were placed (CH_2, C and Si) at different angles and distances, in order to produce ion implantation effects. The implanted substrates were analyzed using the Rutherford backscattering spectroscopy (RBS) at 2.25 MeV alpha particles, to obtain information about the ion dose, ion species and ion penetration range in the implanted substrates. The backscattered alpha particles were collected at 170° and the RBS calibration factor was 2.57 energy/channel. The amount of the implanted or deposited species N_t was calculated by using the following equation [4]:

$$(N_t)_i = \frac{Y_i}{H_M}\frac{Z_M^2}{Z_i^2}\frac{\delta E}{[\varepsilon]_M} \quad (1)$$

where i denotes the implanted species and M is the matrix element, Y_i is the yield of the implanted peak, H_M is the height of signal relative to the matrix element, Z_M^2/Z_i^2 is the ratio between the atomic number of the matrix and the implanted species, δE is the energy resolution in keV/channels and $[\varepsilon]_M$ is the alpha backscattering stopping cross-section factor for the matrix element. The depth t of the implanted species or the deposited thin films was calculated through the following relation [4]:

$$t = \frac{\Delta E}{N[\varepsilon]_M} \quad (2)$$

where ΔE is the alpha energy loss (keV) given by the RBS spectrum and N the matrix density (atoms/cm^3).

The same kind of information can be obtained by irradiating, GAFCHROMIC detector films at INFN-LNS. The GAFCHROMIC is a polymer detector with a high detection efficiency for ions and X-rays. Its darkness increases linearly with the deposited energy of particles and photons.

IPPLM of Warsaw

A Nd:YAg laser with 3 ns laser pulse duration, operating at a 1064 nm fundamental wavelength, 500 mJ pulsed laser energy, single or 1 Hz laser pulses, was employed at IPPLM of Warsaw.

The experimental arrangement at an IPPLM facility, shown in Fig. 1b, was mounted in an interaction vacuum chamber together with a cylindrical accelerating/deflecting electrode connected to a high voltage pulse generator for fast pulsation of the electric field. The target was placed in the front part of the cylindrical chamber and the implanted sample was inside the cylinder at the ground potential. The ions could reach its surface only through two diaphragms [12].

To prevent neutral particles and contaminants from reaching the implanted sample, a large central disc separates the two cylindrical chambers. The distance between the diaphragms placed on the HV box and the grid of the ground tube was about 1 cm. The ions passing through the diaphragm were accelerated by the bias voltage difference formed between the box and the grounded cylindrical electrode. The voltage of power supply was provided by a pulse generator with the period down to 1.5 ms and it ranged from 0 to +30 kV. The accelerating potential was applied to the electrodes with the use of a fast switch at different time delay after the laser pulse.

INFN of Lecce

A KrF excimer laser operating at a 248 nm wavelength, 23–30 ns pulse duration, was used at the LEAS in Lecce, Italy. The laser was a Compex 205 of 600 mJ maximum output energy and 50 Hz repetition rate. The accelerating system was composed of a cylindrical vacuum chamber of 15 cm in diameter. The target was placed inside this chamber and the incidence angle between laser and target was 70° with respect to the normal to the target surface. Figure 2a shows the experimental apparatus. Inside the ground tube (GT) an airtight expansion chamber (EC) was placed tightly closed around the target support of 18 cm in length and 8 cm in diameter. It is connected to a power supply of positive bias voltage. The EC end was drilled by a 1.5 cm hole to allow the ion extraction. In front of it a pierce GE was placed at a distance of 3 cm. After this, another electrode, placed in the drift tube and connected to a power supply of negative bias voltage, was utilized as a third electrode and also as a Faraday cup (FC) collector. It was placed 2 cm from the GE. The laser spot area onto the target surface was about 0.005 cm^2 for all the used laser energies. The third electrode was connected to the oscilloscope by a high voltage capacitor (2 nF), in order to separate the oscilloscope from high voltage, and a voltage attenuator, ×10, in order to set the electric signal to oscilloscope input level. The maximum accelerating applicable voltage was 160 kV [9].

Due to the quite high bias of the third electrode, we were not able to apply the suppressing electrode on the cup and, therefore, the secondary electron emission, caused by the high ion energy, was present. By this configuration, we must be aware to read an output current of about 20% higher than the real one.

Ion implantation of Al and Cu ions in the Si substrates [1], Ge in Si [2] and Ti and C in polyethylene [9] were performed. The analyses on the ion implanted samples were performed by RBS, X-ray photoelectron spectroscopy (XPS) and by the scratch test to determinate the micro-hardness modifictions. Further measurements were performed to estimate, by using the pepper pot method, the transversal emittance value of the plasma emitted ion stream.

LPI of Moscow

For production of beams of accelerated metallic ions at the LPI, the used facility consists of a vacuum diode, Nd: glass laser, operating at a 1.06 μm wavelength in mode-locked regime with 27 ps pulse duration and two pulse energies of 8 mJ or 90 mJ and the ion emission diagnostics as well. The facility was operated at two modes: the first one was intended for studies of ions escaped from the laser produced plasma and the second mode was intended for studies of ions produced with the discharge plasma. The discharge in the diode was initiated with the laser beam focused at the surface of a target serving

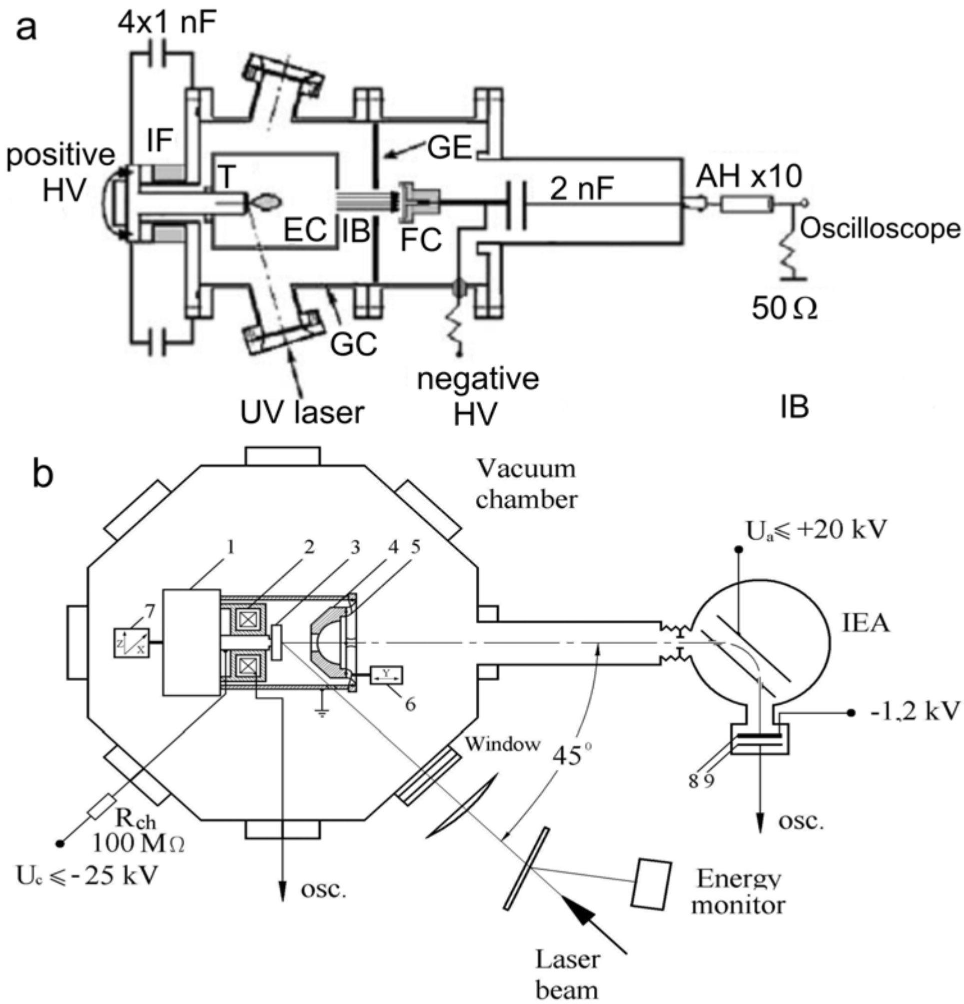

Fig. 2. Sketch of the extraction chamber employed at INFN of Lecce (a) (EC – expansion chamber; IB – ion beam; GE – ground electrode; FC – Faraday cup) and at LPI of Moscow (b) (1 – capacitor; 2 – Rogowski coil; 3 – planar Al target-cathode; 4 – stainless steel anode; 5 – flexible power input; 6 and 7 – movable holders; 8 – microchannel plate; 9 – electron collector).

also as a cathode. Area of the focal spot at the target was of 0.7×10^{-3} cm^2 so that the irradiation intensity was 4×10^{11} W/cm^2 and 4.2×10^{12} W/cm^2. As a target, we used a plate of a pure Al that is placed in a vacuum chamber where the pressure of residual gases was less than 10^{-3} Pa (Fig. 2b). The discharge current was sustained with a capacitor ($C = 0.22$ μF) with a storage voltage up to –25 kV that was connected to the cathode. The total inductance of the discharge circuit was as much as 63 nH and semi-period of the discharge was about of 360 ns. The grounded anode was manufactured of stainless steel, its length was of 1.5 cm and its inner surface was a semi-sphere of 2.2 cm in diameter (Fig. 2b). To provide the ions travelling into the drift tube placed beyond the discharge gap, a hole was made in the anode of 0.6 cm in diameter. The discharge current was measured by a Rogowski coil immediately in the cathode circuit [7]. The charge state spectrum and energy-to-charge ratio of ions escaped from the discharge and the laser produced plasmas are measured by the TOF method with the help of an IEA of the 'plane capacitor' type. The entrance orifice of the analyzer was oriented perpendicular to the target surface and with the aim to enhance sensitivity of the detector we applied a relatively short pass of flight of ions from the target to the analyzer that was of 77 cm. By means varying of biasing of the deflection plates of the IEA, it was possible to measure the ion energy distributions for all ion species.

IEA was used to measure the energy-to-charge ratio of the particles emitted from plasma. The distance target-detector was different in each laboratory: 156 cm at the INFN-LNS; 164 cm at the IPPLM; 77 cm at the LPI), thus the TOF spectra are not directly comparable. By varying the IEA voltage bias of the 90° deflection plates, it was possible to measure the ion energy distributions vs. the ion charge state.

Results

INFN-LNS of Catania

Figure 3a shows a typical TOF spectrum obtained at the INFN-LNS of Catania by ablating a Ti target, with 350 mJ Nd:Yag pulse laser energy and by acquiring with an IC detector placed 56 cm from the target. The TOF peak is located at 30 μs; this corresponds to the Ti ion energy of 675 eV. By knowing the input resistance of 1 MΩ of the used fast storage oscilloscope, it is possible to have an estimation of the implanted ion dose by considering the total current of the IC signal. The

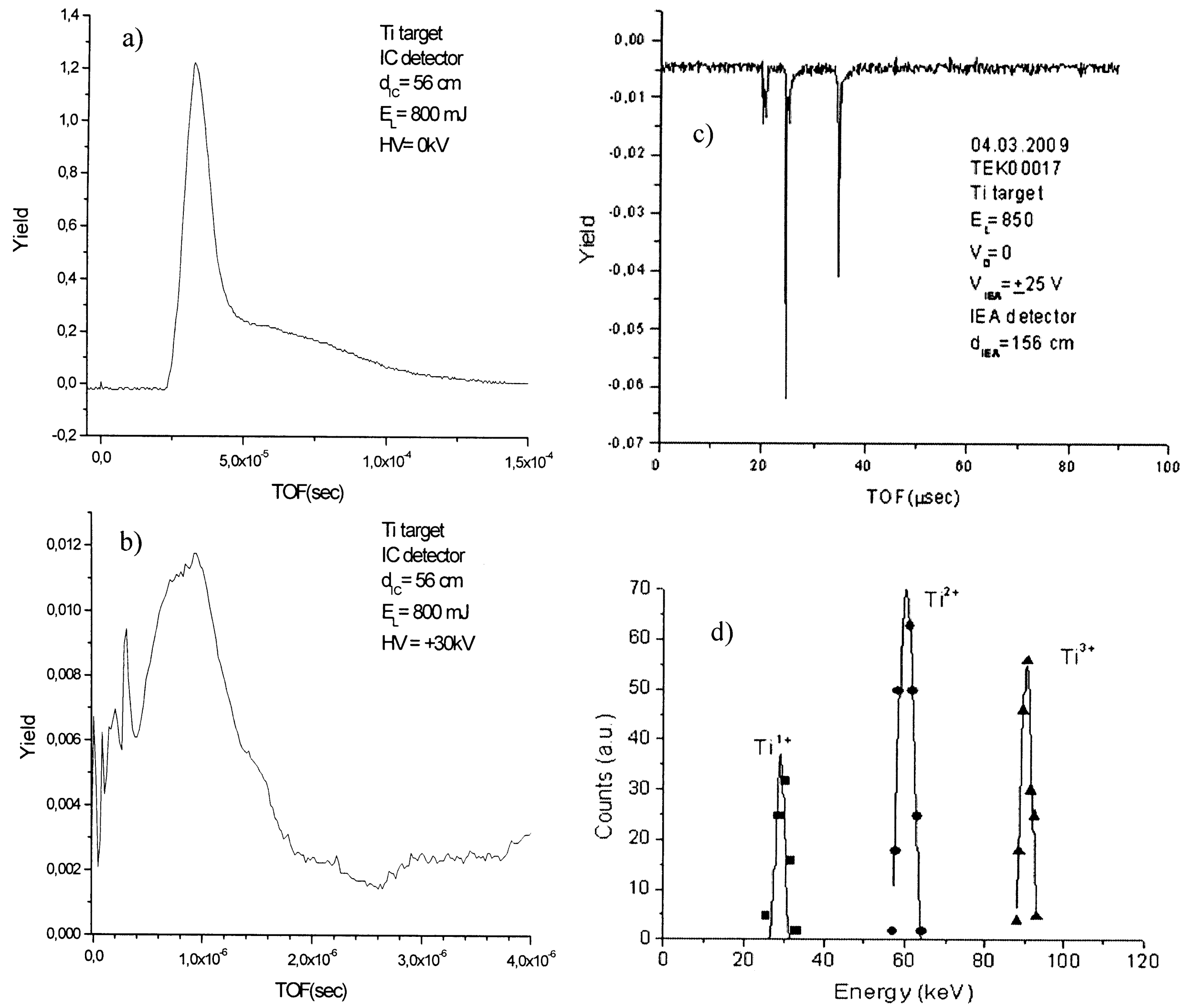

Fig. 3. Typical IC-TOF spectrum, obtained by ablating Ti target with 350 mJ pulse laser energy at a distance IC-target of 56 cm at INFN-LNS, without post acceleration (a) and by using +30 kV voltage post acceleration (b). Typical IEA-TOF spectrum obtained without the post-acceleration system, showing 3 charge states for the Ti ions (c). Experimental ion energy distributions obtained by using +30 kV of post acceleration (d). The three distributions were fitted by using a Gaussian curve.

measured value is 10^9 Ti particles/pulse. Considering an exit spot surface from the post-acceleration system of 0.5 cm^2, the total ion dose per hour was found to be 7.2×10^{12} ions/(cm^2 hour). For comparison, Figure 3b shows the TOF spectrum obtained by using +30 kV voltage. In this case the spectrum is shifted toward lower TOF because the ions are faster. In particular, the TOF peak now is located at 1.1 μs, corresponding to a mean energy value of 62 keV.

Figure 3c reports a typical IEA spectrum of the Ti ions emitted from a target irradiated with a 350 mJ pulse energy at the INFN-LNS. The spectrum shows the ions detected with a bias of the plates of ±25 V. By varying the voltage bias of the plates, it is possible to know that in such conditions the maximum charge state of Ti ions is 3+. By changing the bias of the deflection plates, it is possible to analyze the different energy-to--charge ratio, so that the ion energy of the three charge states can be measured. Figure 3d shows the experimental ion energy distributions obtained by using +30 kV of post-acceleration system. The three experimental peaks were fitted by using a Gaussian curve; the peaks are shifted towards higher energies when the charge state increases. The three distributions are peaked at 30, 60 and 90 keV in the case of Ti^{1+}, Ti^{2+} and Ti^{3+}, respectively. The energy resolution $\Delta E/E$ is 10, 8 and 4% for Ti^{+}, Ti^{2+} and Ti^{3+}, respectively.

IPPLM of Warsaw

Figure 4 shows the TOF spectrum obtained at the IPPLM by an ion collector which was located on the axis of the grounded electrode at a distance of ~30 cm from the target (7 cm from the grid) together with the HV gating signal. Recording of such spectra allowed for characterization of the parameters of the ion streams, namely their energy (based on the TOF) and relative concentration (based on the integrated ion current). In Fig. 4 due to application of the accelerating voltage, the laser induced ion pulse was chopped into 10 short ion pulses which full width and half maximum (FWHM) was measured as 140 ns. Due to the geometric features of the set-up, the ion pulses were delayed in respect to the HV pulses approximately by 1.2 μs. The target was irradiated by a laser pulse of energy

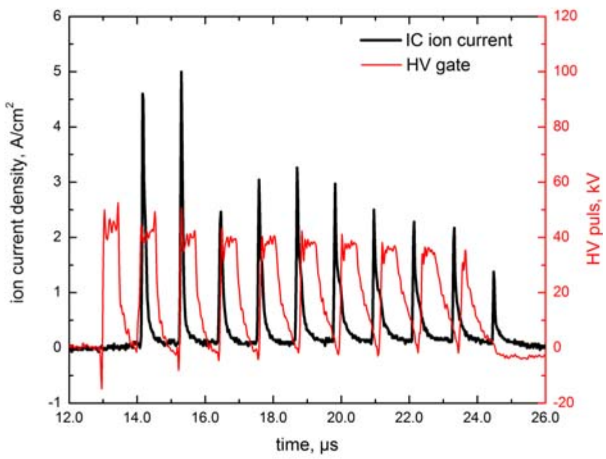

Fig. 4. IC spectrum obtained with the post-acceleration system at IPPLM.

500 mJ. In this case the obtainable total ion dose emitted from the target was 6.4×10^{14} ions/(cm^2 hour). For the optimized system parameters (amplitude –40 kV, delay 10–14 μs), i.e. allowing for the achievement of the highest ion signal and the best filtration of contamination [13], *quasi*-monoenergetic ion groups of energy in the range of 10 keV were obtained. This would not be possible in a standard set-up based only on a direct implantation method (with average ion energy lower than 1 keV). The application of the acceleration/deflection system not only made it possible to obtain higher energy and narrower energy distribution of ions but also was demonstrated to be useful for filtering out contaminations.

INFN of Lecce

Figures 5a and 5b show typical TOF spectra obtained at the INFN of Lecce by irradiating a Cu target and by detecting the ion emission with an IC placed 23 cm from the target. The laser energy was 11 and 17 mJ deposited onto a spot of 0.005 mm^2 for Figs. 5a and 5b, respectively. A comparison between the IC spectra with different post ion acceleration values is reported in both figures.

The vertical axis represents the output signal in volts. The corresponding current is obtained dividing the voltage values per 50 Ω and multiplying to the attenuator coefficient, ×10. By these figures, one can observe that the space charge domination effects are present at high laser energies and low accelerating voltages. At highest laser energy, more easily high plasma density is reached and breakdown processes short circuit the anode. Thus, considering the peak values of only curves out of the charge domination effects and break down processes, we obtain the behaviour of the accelerated charge on the accelerating voltage (Figs. 5c and 5d). From these

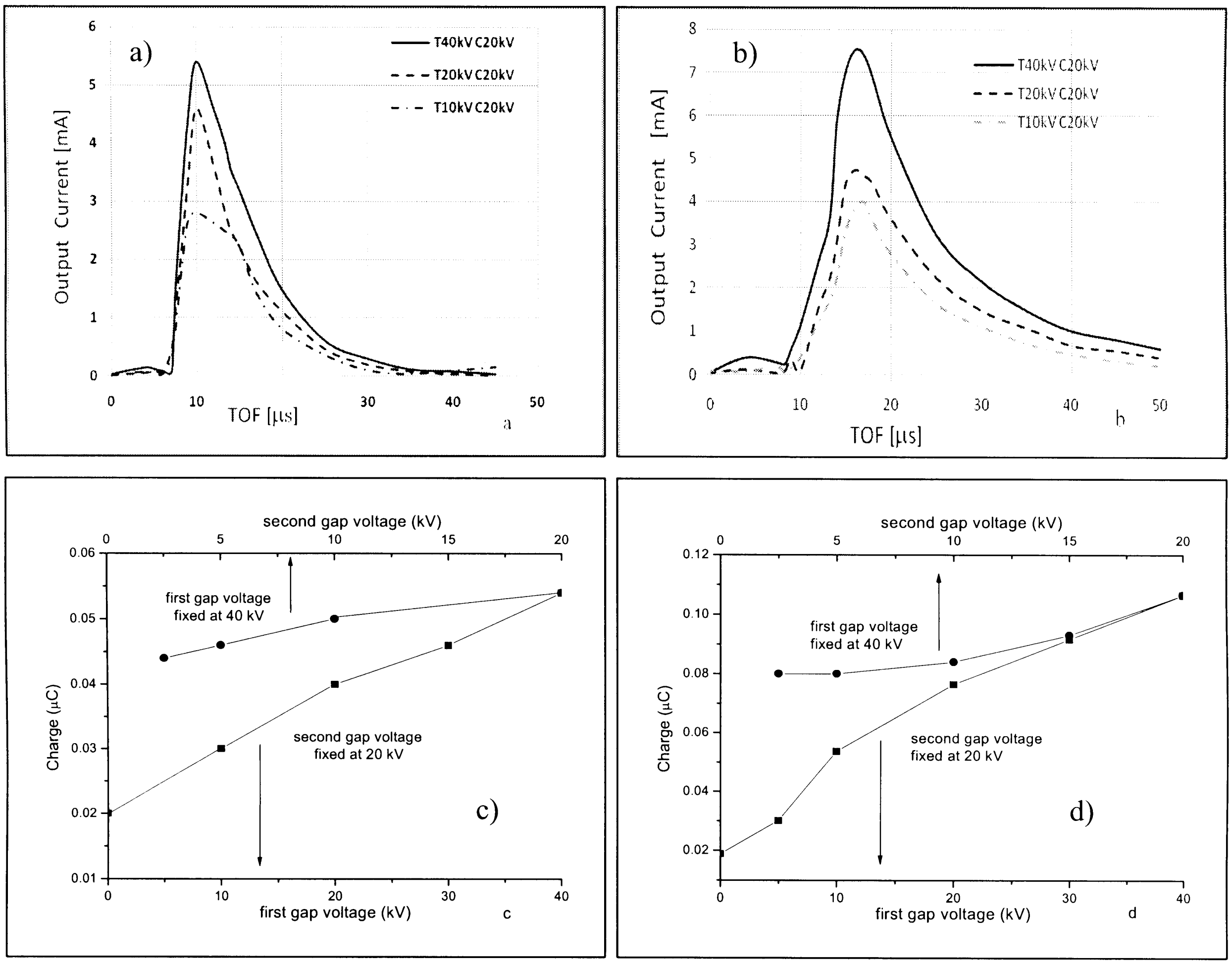

Fig. 5. Typical TOF spectra and output charge obtained at INFN of Lecce by irradiating a Cu an a Y target. Cu (a) and Y (b) spectra at three pairs of applied voltage; Cu (c) and Y (d) output charge on voltage applied to the target and cup.

results we can observe the absence of the saturation phase. In fact both curves of Figs. 5c and 5d have a growing trend and the ones dependent on the first acceleration gap are higher than the ones dependent on the second acceleration gap.

Theoretically, it is expected to see a constant trend for the curves dependent on the second acceleration gap because the charge is already extracted and its value ought to be stable. Then, the observed behaviour can be ascribed to the secondary emission of electrons from the cup collector that we do not able to prevent owing to the absence of the suppressing electrode on the FC. So we expect that the charge detected by the cup grows with voltage increasing by about 20% for the used voltages.

The current increased on the first gap voltage and the slope was higher (150%) than the one of current curve dependent on the second gap voltage. This result implies a strong dependence of the extraction efficiency with the first stage voltage. Since the anode consists of a cylinder with a hole at its end (1.5 cm in diameter) in order to escaping the ions, (Fig. 3a), the electric field strength near the hole increased with applied voltage. This behaviour enlarged the extracting volume inside the anode and, as a consequence, the extraction efficiency [8].

LPI of Moscow

Figure 6a depicts the Al ion energy distributions for selected ion species obtained by the IEA for ions escaping from the plasma produced with a laser pulse of energy 90 mJ and corresponding power density of 4.2×10^{12} W/cm^2. Figure 6b depicts the same event for ions escaped from a micropinch that is produced within plasma of moderate energy vacuum discharge (stored energy of 600 mJ) initiated at the inter-electrode gap by a laser pulse of 8 mJ energy (i.e. power density of 4×10^{11} W/cm^2). One can see that the typical energy distribution for the laser produced plasma is of a near Maxwellian shape and the maximum ion energies exceed 60 keV. Nevertheless, energy distributions of ions from the discharge plasma exhibit significant non-Maxwellian tails of the accelerated ions that suggests the presence of an additional non-thermal acceleration mechanism. Note, that a similar shape of energy distribution was obtained earlier for ions escaped from micropinches produced at plasma jet of the electrically initiated low voltage vacuum spark [17].

The ranges of kinetic energies for all ion species Al^{n+}, which are measured with the use of IEA are presented in Figs. 6c and 6d. The thin lines in Figs. 6c–6d

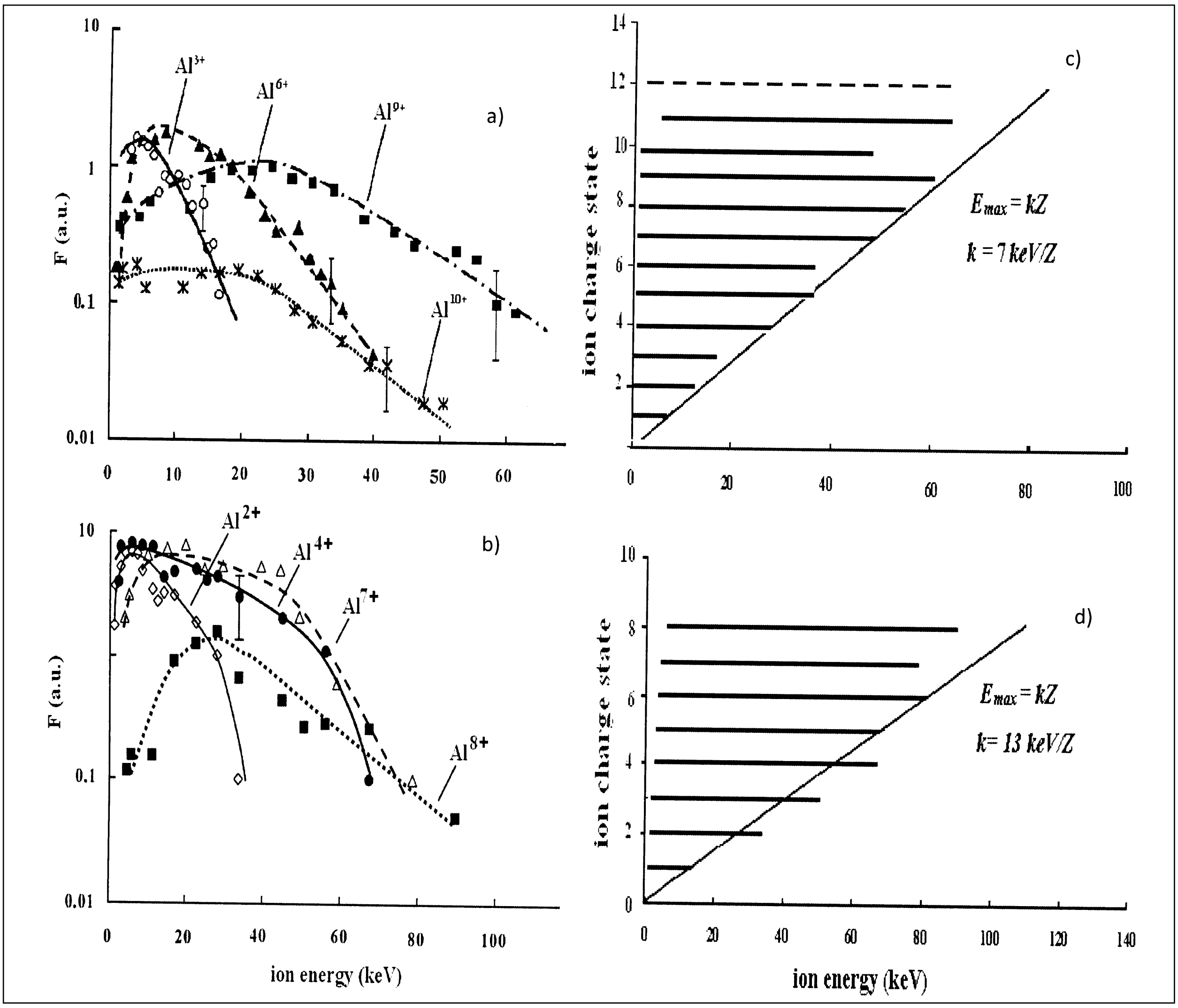

Fig. 6. Energy distributions (left column: (a), (b)) and ranges of kinetic energies (right column: (c), (d)) for the selected species of Al^{n+} ions escaped from the laser produced (a) and the micropinch plasmas (b), which are measured with the use of IEA.

depict the linear fit $E_{max} = kZ$ for maximum energies of ions escaped from both the laser produced and from the micropinch plasmas. One can see that the latter grows near two times steeper that the first one and attains about 80 keV for the ions Al^{6+}–Al^{8+}. This acceleration results in the acceleration of ions of the target up to energies of 13 keV/charge state.

The post ion acceleration is a technique which permits to generate ion beams of special interest in the field of ion implantation. The advantages presented by the post ion acceleration technique consist in the relative low cost of the system, in the high current obtainable and in the use of ions at different energy which can be implanted simultaneously at different depth in the substrate. At high doses, the implants can modify significantly the chemical and physical properties of many materials. The control of the implanted dose can be obtained theoretically, using SRIM code [3] and experimentally, using the RBS analysis [4].

Figures 7a and 7b show some results obtained with the 2.25 MeV alpha particle RBS analysis of the Ge ions implantation of Si substrates at a dose of about

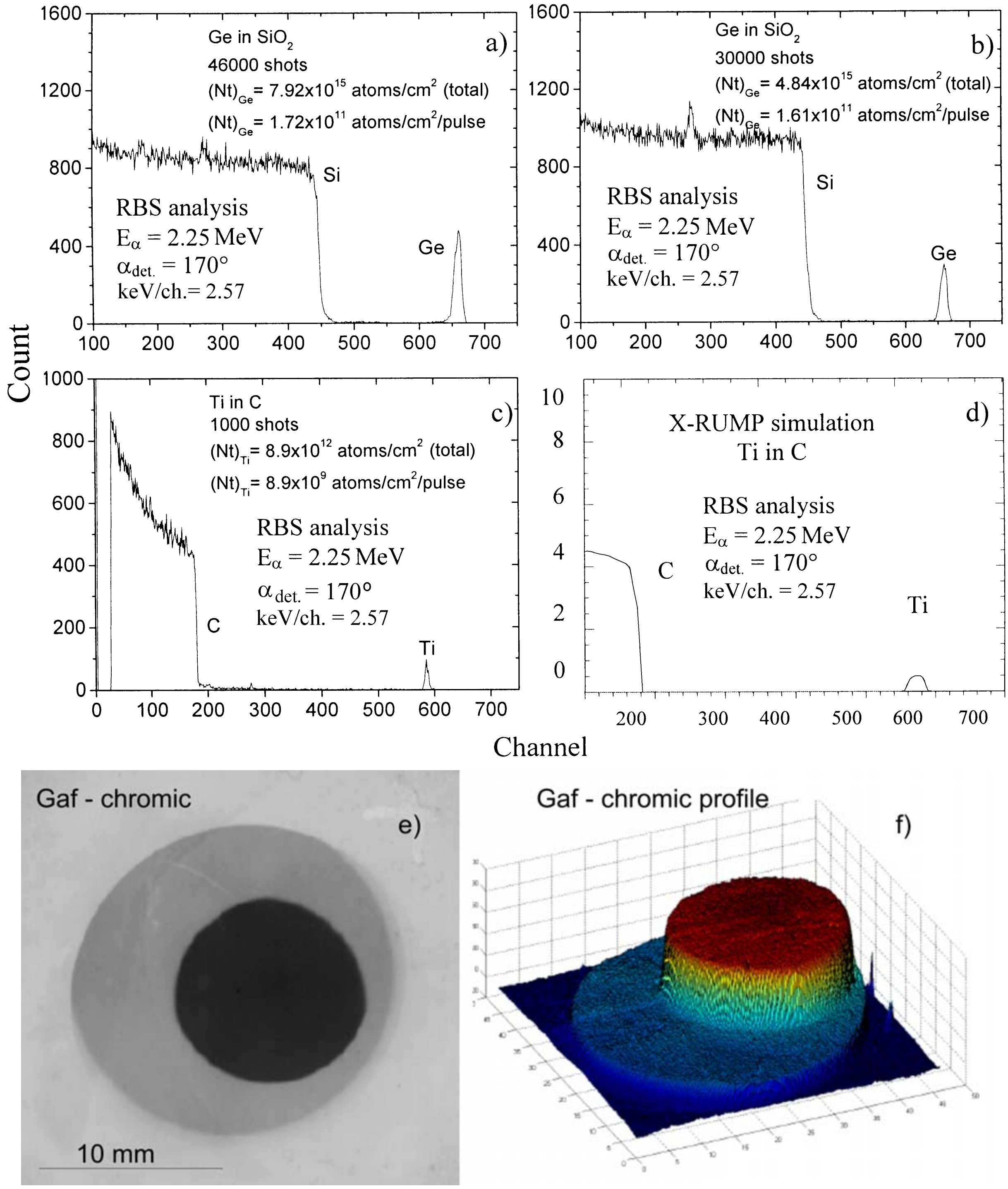

Fig. 7. RBS spectra of Ge implanted in SiO_2 substrate (a, b) and of Ti implanted in C substrate (c). For comparison, the relative X-RUMP simulations (d) is also reported. Ti implantation of a GAFCHROMIC film (e), where it is possible to distinguish the black zone corresponding to the X-ray and ion irradiation and a light zone corresponding only to the ion implantation. The last figure (f) shows the GAFCHROMIC darkness spatial profile.

8×10^{15} and 4×10^{15} atoms/cm^2, respectively, by means of the system with post acceleration at IPPLM. The experimental spectrum shows that the Ge ions are implanted up to 50 nm depth, i.e., on the basis of the Ge energy loss, the corresponding kinetic energy of Ge ion is 65 keV. This result is also in agreement with the SRIM simulation code of Ziegler [3]. The same figure reports the RBS spectrum relative to the Ti implantation in a C substrate (Fig. 7c) and, for comparison, the relative RBA X-RUMP simulation (Fig. 7d). This last experimental spectrum demonstrates that in the case of Ti implantation in carbon the penetration depth is 40 nm and the corresponding kinetic energy, taking into account the Ti energy loss, is 50 keV. In this case the implanted ion dose is about 9×10^{12} atoms/cm^2.

Another implanted substrate was the GAFCHROMIC detector film, which was implanted by Si, Ti, Ge, C and H ions. This polymeric detector consists of a clear transparent polyester film covered by a thin (6 μm) sensible GAFCHROMIC polymer sensitive to ionizing radiations [11]. UV, X-rays, electrons and ions induce darkness in the sensible polymer proportionally to their deposited energy in the active layer.

The result of a typical exposition is reported in Fig. 7e. This photo shows a large spot light due to the ion implantation and a concentric spot, more dark, due to the detection of X-rays. The two spots are not concentric, due to the 45° laser incidence angle on the target and to the different ions and X-ray focus inside the plasma. In this case the detector was placed 100 cm from the extraction chamber. The ion spot diameter is about 10 cm and the corresponding total angular aperture of the post accelerated Ti ions is about 6°. Figure 7f shows the GAFCHROMIC darkness intensity spatial profile optically measured.

Discussion and conclusions

The post ion acceleration of ions emitted from laser-generated plasma can be developed with different methods, as presented in this article by the four different European laboratories. The comparison of the four techniques demonstrates that each of them has advantages and disadvantages.

The INFN-LNS method has the advantage to accelerate ions along the axis normal to the lasered target surface up to 30 keV/charge state. This permits to use an ion diagnostics very simply by placing it along this direction or by putting, at a given distance, a substrate to be ion implanted. The post accelerated ions have a spot of about 1 cm^2 and they are of the order of 10^9 particles/pulse, thus by using 10 Hz repetition rate and 1 h laser irradiation the implantable ion dose is of about 3.6×10^{13} ions/cm^2, a value useful to modify the surface properties of many polymers. The doses need to modify physically and chemically the surface of many metals is of the order of 10^{16} ions/cm^2, thus for the low extracted currents this post acceleration method is not advantageous.

The IPPLM method has the advantage to avoid ion implantation of neutrals and nanometric and micrometric debris. Moreover, the experimental apparatus permits to deliver at 30 kV dose rates higher, up to near two orders of magnitude with respect to the value obtained at LNS facility, permitting to implant high ion doses in a relatively low time.

The INFN of Lecce method has the advantage to obtain very high acceleration energies. The system and the used power supply permit to accelerate ions up to 140 keV/charge state. Thus for elements with six charge states, obtainable for Cu as an example, the kinetic energy can reach 840 keV.

The LPI of Moscow has the advantage to accelerate up to about 13 keV/charge state, obtaining for the six charge states of Cu a maximum energy of 78 keV. In this case a low energy plasma pulse is applied for initiation of a vacuum spark. If parameters of the laser pulse are optimized, as well, so that to provide production of a micropinch within the cathode plasma flame, then the multiple charged ions, which are produced within the micropinch, are post accelerated by the self-consistent electric field. The field, if generated, with the self-consistent ambipolar electric field that is arisen by beams of fast electrons running away the hot plasma of the micropinch. By comparison of the results presented in Figs. 6a and 6b, one may conclude that post acceleration of multiple charged ions in self-consistent electric field produced at plasma of micropinch permits to approach significant ion energies at the very moderate power contribution. The other advantage of this method is that it does not require a special high voltage facility. Nevertheless, this method has a disadvantage that the accelerated ions have rather extended energy distribution, compared to ions accelerated by the external electric field (Fig. 3d), so that the method is usable just for a limited range of challenges (hardening of tools by ion implantation, for instance, etc.).

Works are in progress in order to optimize the different acceleration methods and in order to compare better many parameters of the multi-energetic and multi-species ion beams, in terms of energies and energy spreads, current vs. charge state, repetitive pulse ion beams, emittance beams, spot diameters, etc.

References

1. Belloni F, Doria D, Lorusso A *et al*. (2005) Characterization of ablation plasma ion implantation. Nucl Instrum Methods B 240:36–39
2. Belloni F, Doria D, Lorusso A, Nassisi N, Krasa J (2006) Pre- and postextraction analyses of different charge state ion components produced in a laser ion source. Rev Sci Instrum 77:03B301
3. Biersak JP, Ziegler JF (2011) Genplot and RUMP, http://www.lightlink.com/genplot/download.htm
4. Feldman LC, Mayer JW (1986) Fundamentals of surface and thin film analysis. North-Holland Publishing, New York
5. Gammino S, Torrisi L, Celona L *et al*. (2008) Perspectives for the ECLISSE method with third generation ECRIS. Radiat Eff Defects Solids 163;4/6:277–286
6. Hegelich BM, Albright BJ, Cobble J *et al*. (2006) Laser acceleration of quasi-monoenergetic MeV ion beams. Nature 439;26:441–444
7. Korobkin YuV, Paperny VL, Romanov IV, Rupasov AA, Shikanov AS (2008) Micropinches in laser induced moderate power vacuum discharge. Plasma Phys Controlled Fusion 50:065002

8. Lorusso A, Siciliano MV, Velardi L, Nassisi V (2010) Double acceleration of ions and application in biomaterials. AIP Conf Proc 1209:79–82
9. Lorusso A, Siciliano MV, Velardi L, Nassisi V (2010) Low emittance plasma ions beam by a new double accelerating configuration. Nucl Instrum Methods A 614:169–173
10. Nassisi V, Pedone A (2003) Physics of the expanding plasma ejected from a small spot illumined by an ultraviolet pulsed laser. Rev Sci Instrum 74:68–72
11. Niroomand-Rad A, Blackwell CR, Coursey BM *et al*. (1998) Radiochromic film dosimetry: Recommendations of AAPM Radiation Therapy Committee Task Group 55. Med Phys 25;11:2093–2115
12. Rosinski M, Paris P, Wolowski J, Gasior P, Pisarek M (2010) Electrostatic acceleration and deflection system for modification of semiconductor materials in laser--produced ion implantation. Radiat Eff Defects Solids: Plasma Science & Plasma Technology 165:528–533
13. Torres R, Vervisch V, Halbwax M *et al*. (2010) Femtosecond laser texturization for improvement of photovoltaic cells: black silikon. J Optoelectron Adv Mater 12;3:621–625
14. Torrisi L, Caridi F, Giuffrida L (2010) Comparison of Pd plasmas produced at 532 nm and 1064 nm by a Nd:YAG laser ablation. Nucl Instrum Methods Phys Res B 268:2285–2291
15. Torrisi L, Caridi F, Margarone D, Picciotto A, Mangione A, Beltrano JJ (2006) Carbon-plasma produced in vacuum by 532 nm–3 ns laser pulses ablation. Appl Surf Sci 252:6383–6389
16. Torrisi L, Gammino S, Andò L, Laska L (2002) Tantalum ions produced by 1064 nm pulsed laser irradiation. J Appl Phys 91;5:4685–4692
17. Zverev EA, Krasov VI, Krinberg IA, Paperny VL (2006) Micropinches in plasma flame expanding into vacuum ambient. Czech J Phys 56;Suppl 2:B324–B334